

# Test of 60 kA coated conductor cable prototypes for fusion magnets

D Uglietti, N Bykovsky, K Sedlak, B Stepanov, R Wesche and P Bruzzone

Ecole Polytechnique Fédérale de Lausanne (EPFL), Swiss Plasma Center (SPC), CH-5232 Villigen PSI, Switzerland

## Abstract

Coated conductors could be a promising material for the fabrication of large magnet systems of future fusion devices. Two prototype conductors (flat cable in steel conduit) each about 2 m long were manufactured using coated conductor tapes (4 mm wide) from Superpower and Superox, with a total tape length of 1.6 km. Each flat cable is assembled with 20 strands, each strand consisting of a stack of 16 tapes surrounded by two half circular copper profiles, twisted and soldered. The tapes were measured at 12 T and 4.2 K and the results of the measurements were used for the assessment of the conductor electromagnetic properties at low temperature and high field. The two conductors were assembled together in a sample that was tested in the European Dipole (EDIPO) facility. The current sharing temperatures of the two conductors were measured in background fields from 8 T up to 12 T and for currents from 30 kA up to 70 kA: the measured values are within few percent from the values expected from the measurements on tapes (short samples). After electromagnetic cycling  $T_{cs}$  at 12 T and 50 kA decreased from about 12 K to 11 K (about 10%), corresponding to less than 3% in  $I_c$ .

Keywords: fusion cable, coated conductor cable, fusion magnet, HTS cable

## 1. Introduction

Cables with current capacity of tens of kA in background fields of over 10 T are required for the construction of large fusion magnets. Traditionally cable-in-conduit conductors manufactured with Nb<sub>3</sub>Sn and NbTi round wires have been used, for example for the ITER magnet system [1].

There is a growing interest in using High Temperature Superconducting (HTS) materials for preparing large current conductors for fusion magnets [2]. HTS materials, and coated conductors in particular, could have several advantages with respect to LTS wires. First of all, the operating temperature could be higher than the one for Low Temperature Superconducting (LTS) materials, which is usually around 5 K; furthermore the HTS materials can be operated also at field much higher than LTS, even if the management of the electromagnetic forces on the magnet assembly becomes the main challenge. Coated conductors are relatively new on the market (less than 15 years), thus they still have a much larger margin of improvements compared to the “older” Nb<sub>3</sub>Sn and NbTi. Despite the high cost of coated conductors, which at present makes most of the applications non-competitive against existing copper or LTS, low cost fabrication routes are investigated, with an ultimate target of achieving a price lower than the one of Nb<sub>3</sub>Sn wires.

Among HTS materials, only Bi2212 is available in round wires; in contrast with LTS, REBCO and Bi2223 are available only in tapes with high aspect ratio. Therefore most of the effort has gone into the development of cable designs compatible with tapes. Various concepts have been proposed in the last few years (for example [3-5]), but

only the stacked conductor concept, with non-transposed tapes, has so far demonstrated large currents, with a critical current exceeding 67 kA at 4.3 T and 45 K [6]. Such non-transposed conductor is suitable only for Heliotron type magnets, because of the very short conductor length ( $< 20$  m) between two joints, but it cannot be used for tokamaks, which should be built with long length ( $> 1$  km) conductors with fully or partially transposed strands; these conductors should also be manufactured at low cost at industrial scale.

At the Swiss Plasma Center (SPC, remained from CRPP in October 2015) the stacked strand concept, first introduced by the Massachusetts Institute of Technology [3], was selected because of the simplicity of manufacturing and the flexibility in design parameters. The activities on cable development started in 2012 with the preparation and test of preliminary soldered and twisted stacked strands [7] using 3 mm wide tapes and simple copper profiles; bending tests were performed at 77 K for determining the minimum bending radius. General considerations on cable design were presented in 2013 [8] together with the electromechanical test of a first strand type (4 mm wide tape, 6.2 mm diameter) that was going to be used for the cable prototypes. The design and manufacturing of the cable prototypes were presented in [9]; in the same paper possible designs for fusion cables using Bi2212 wires and Bi2223 tapes were introduced. Advanced strand designs and optimization of the cable parameters have been discussed in detail in [10]. This paper reports the assembling of the prototype cables into a sample to be measured in the EDIPO facility; the results of the test campaign includes current sharing temperature ( $T_{cs}$ ), critical current ( $I_c$ ), AC losses and their evolution during electromagnetic cycling.

## 2. Design of the prototype

When operated at low temperatures (around 5 K) the main difference in physical properties between classical LTS materials and REBCO is the much higher critical temperature and critical field of the latter. The critical current normalized at 4.2 K and 12 T is plotted in figure 1 for an ITER type Nb<sub>3</sub>Sn wire (at -0.35% intrinsic strain) and for a coated conductor tape (data from [11], field perpendicular to the wide face of the tape). From figure 1 four distinctive features of coated conductors can be identified. First, while Nb<sub>3</sub>Sn must be operated at low current (around 50% or 60% of  $I_c$  at 4.2 K) in order to get a sufficient temperature margin (at least 0.5 K), coated conductors could be operated relatively close to  $I_c$  (for example at 80% or 90% of  $I_c$  at 4.2 K), retaining a comfortable temperature margin; therefore less material would be needed for the fabrication of cable with a certain current capacity because the coated conductors can be used almost at full potential. Second, in coated conductors any improvement in  $I_c$  (which is achieved from the tape manufacturers) would be more effective in increasing  $T_{cs}$  than improvements in  $I_c$  in Nb<sub>3</sub>Sn wire: for example a gain of 10 % in  $I_c$  in coated conductors could lead to an increase in  $T_{cs}$  of 25% (about 2.5 K in figure 1), while the same improvement in the  $I_c$  of Nb<sub>3</sub>Sn would lead only to a modest 3% improvement in  $T_{cs}$  ( $< 0.5$  K in figure 1). Third, a relatively large transition from superconducting to normal state is expected when the temperature crosses  $T_{cs}$  at constant current. Fourth, a consequence of the shallow transition in temperature is that in HTS small errors in the measurement of  $I_c$  brings large error in the estimation of  $T_{cs}$ ; therefore a  $T_{cs}$  measurement (temperature ramps at constant current) would be more sensitive to probe the transport properties than an  $I_c$  measurement (current ramp at constant temperature).

The main objective of the construction and test of the cable prototypes is the demonstration of current capacity in the same range as ITER/DEMO cables, i.e. currents of at least 50 kA in background field of at least 10 T. The tapes in the cable should be partially transposed and a large copper cross section ( $> 500$  mm<sup>2</sup>) is also required because of the long

time constant of the magnet system during discharge. In order to satisfy these requirements it was decided to use 320 tapes per cable, which should guarantee operating currents of more than 50 kA. The tapes were arranged in 20 strands each containing 16 stacked and twisted tapes; the twist pitch at strand level was set at 320 mm. The twist pitch at cable level (i.e. the twist pitch of the strands cabled around the copper core) is 1000 mm; this twist pitch together with a core thickness of 5 mm limit the peak strain in the tapes at the cable edge to less than 0.5% (see [10] for details).

Cable cross-sections (excluding the steel jacket) and transport parameters of the cable are reported in table 1 together with the corresponding values for the ITER Toroidal Field (TF) cable and for a prototype DEMO TF cable [12]. Even if the coated conductor cable prototypes have a current somehow smaller than ITER or DEMO Nb<sub>3</sub>Sn cables, a modest increase in the number of tapes (or an improvement in  $I_c$ ) is sufficient to match the current capacity of the ITER/DEMO cables. Probably the total copper cross section of the HTS prototype cable is over dimensioned and it should be further optimized, also taking into account the peculiar behaviour of coated conductors during quenches [13].

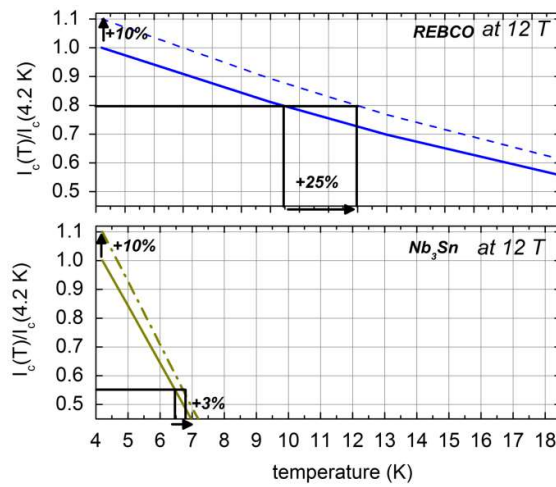


Figure 1. Reduced critical current versus temperature at 12 T (magnetic field perpendicular to the wide face of the tape) for a coated conductor (top;) and for a Nb<sub>3</sub>Sn wire (bottom). Assuming  $I_{op}=0.8 \cdot I_c$  for the coated conductor and  $I_{op}=0.55 \cdot I_c$  for the Nb<sub>3</sub>Sn wire, in case of an improvement of 10 % of  $I_c$  at 4.2 K, the improvement in  $T_{cs}$  would be 25% for the coated conductor and 3% for the Nb<sub>3</sub>Sn wire.

	Tot. cross section without jacket	Tot. copper cross section	Void fraction	Operating current and field	$T_{cs}$ at operating conditions	Operating current density (non-Cu)
<b>ITER TF (Nb<sub>3</sub>Sn)</b>	1250 mm <sup>2</sup>	515 mm <sup>2</sup>	400 mm <sup>2</sup> (32%)	68 kA, 11.1 T	6.1 K to 7.5 K	280 A/mm <sup>2</sup>
<b>DEMO TF (Nb<sub>3</sub>Sn)</b>	1220 mm <sup>2</sup>	675 mm <sup>2</sup>	280 mm <sup>2</sup> (23%)	82 kA, 13.4 T	about 6.5 K	300 A/mm <sup>2</sup>
<b>HTS prototype (this paper)</b>	1250 mm <sup>2</sup>	760 mm <sup>2</sup>	400 mm <sup>2</sup> (32%)	50 kA, 12 T 30 kA, 12 T	8 K 21 K	500 A/mm <sup>2</sup> 300 A/mm <sup>2</sup>

Table 1. Total cross section, copper cross section and void fractions for ITER TF cable (in production), DEMO TF cable (prototype) and the HTS cable discussed in this paper; the steel jacket is not taken in consideration. The transport properties are reported at 0.1  $\mu\text{V}/\text{cm}$ .

### 3. Fabrication of the prototype

The whole fabrication process of the two conductors was carried out at laboratory scale (a detailed description of the cable design and manufacturing can be found in [9]), but there should be no technological obstacles preventing an industrialization. The tapes (1.56 km in total, about 780 m per sample) were purchased from Superpower for one cable and from Superox for the second cable.

The strands (6.2 mm in diameter) were prepared by stacking the tapes between two semi-circular copper profiles, twisting and passing through a solder bath (eutectic PbSn) to solder all the components together. Each set of 20 strands was cabled around a flat copper core. Design dimensions of the copper core were 5 mm x 50.9 mm, but in case of the Superpower cable a copper core 55 mm wide and 5 mm thick was used: the size was a bit larger than the actual space required for arranging all the 20 strands, because it was unclear whether the required tolerance should be kept large or small. Indeed after cabling all the strands there were relatively large gaps between the strands; therefore copper strips 0.5 mm thick and 6 mm wide were inserted between the strands in order to fill up the voids and limit the strand movements under electromagnetic forces. When the Superox cable was prepared the copper core was machined down to 51.5 mm, and the strands were placed around the core without any gap.

For both tape manufacturers the  $I_c$  of the tapes was not the same in all the spools (production batches) that were purchased; from Superpower 23 different spools (corresponding to production batches) were purchased while for Superox four spools were purchased (see next section). In order to obtain uniform critical current among the strands, the tapes were distributed among the strands according to their individual critical currents at 4.2 K, 12 T: 320 tapes were distributed in 20 strands, such that the standard deviation of the strand  $I_c$  is about 1% for the Superpower strands and about 0.02% for the Superox strands, even if the standard deviation of the  $I_c$  was 20% among the Superpower spools and 5.5% among the Superox spools. Average expected critical currents of the Superpower / Superox strands are 1160 A / 1600 A at 77 K, 0 T (including self-field effect, see [14]) and 3104 A / 3112 A at 4.2 K, 12 T; at 77 K and self-field the variation in  $I_c$  among the strands of the same manufacturer is of course larger than the one at 4.2 K, 12 T because the tapes were distributed among the strands based on the values of  $I_c$  at 4.2 K, 12 T. The critical current of all the strands was measured in liquid nitrogen just after the fabrication (the strands were straight) and, for some of them, after cabling (strands were bent around the edge of the flat copper core) as intermediate verification stages: for the Superpower cable seven strands were measured after cabling while for the Superox cable ten strands were measured; the critical current values normalized to the expected ones are plotted in figure 2. The  $E-I$  curves before and after cabling for three strands of each manufacturer are plotted in figure 3. For both manufacturers the  $I_c$  at 77 K of the straight strands (in grey in figure 2) is slightly lower than the expected values (up to 3% lower for Superox and up to 8% lower for Superpower), probably because of the field dependence of  $I_c$  at 77 K; the peak magnetic field perpendicular to the wide face of the tapes was 140 mT for the Superpower strands and 165 mT for the Superox strands. For both manufacturers a systematic increase (less than 4%) in  $I_c$  is observed after the strands are cabled: further tests will be carried out in order to understand the reason.

After the tests at 77 K each cable was enclosed in a rectangular steel jacket (3.5 mm thick on the wide side and 2 mm thick on the narrow side); the jacket is composed of two machined steel profiles welded around the cable. A photograph of the cross section of a trial assembly (with an aluminium jacket) is shown in figure 4a. Tests were carried out to verify that during welding the temperature of the strands does not exceed the melting temperature of the solder alloy (188° C); a thermocouple inserted in a dummy strand measured a maximum temperature of less than 100° C. In figure 4b a 3D model of the conductor (copper core, strands and steel jacket) is presented.

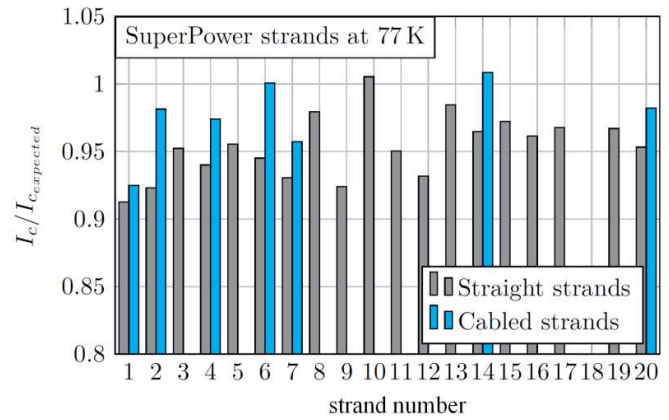
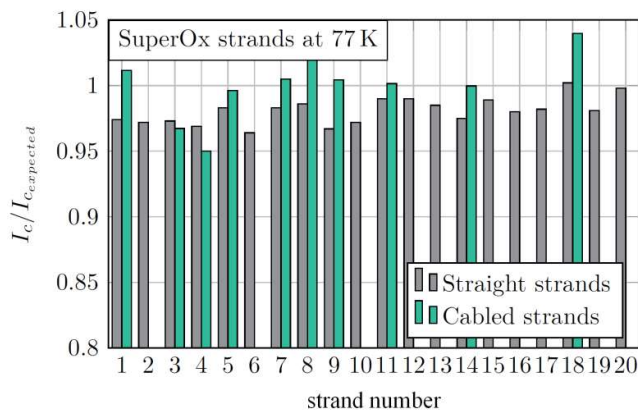


Figure 2. Ratio between measured and expected critical current for the strands made with Superox (left) and Superpower tapes (right); the distance between the voltage taps was 150 cm. The grey bars are for the  $I_c$  measured on straight strands, while the green/blue bars are for the  $I_c$  measured on cables strands.

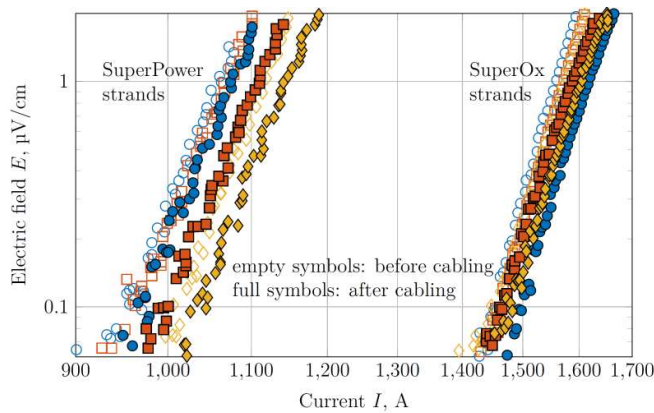


Figure 3. Electric field versus currents for three Superpower and Superox strands, measured before and after cabling.

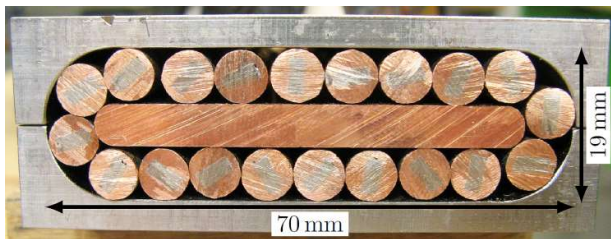


Figure 4a. Photograph of the cross section of a trial conductor: the jacket is made with aluminium and it is slightly thicker than the actual jacket used for the conductors.

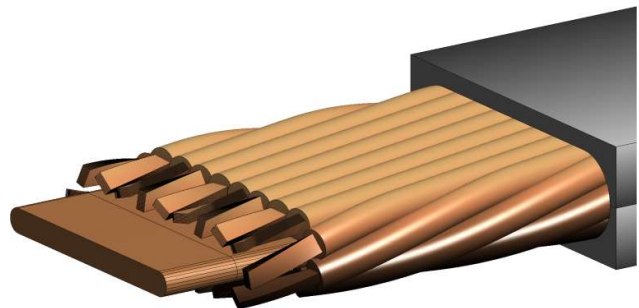


Figure 4b. 3D model of the conductor

The terminations of the conductors should satisfy electrical and geometrical requirements. For the operation up to 100 kA of the superconducting transformer in the EDIPO facility the total resistance of the whole circuit, including all the joints and terminations between the transformer, the HTS adapter (which is required to connect the HTS sample with the superconducting transformer) and the HTS conductors must be less than 10 nΩ. In addition the terminations of the cable prototypes should fit in the narrow space available at the HTS adapter end. The strands were prepared

with the tapes longer than the copper profiles, and the tapes were staggered at the ends of the strands (see figure 5) so that each tape is in contact with the copper of the termination over 15 mm. Each termination consists of a copper block with 10 grooves (3 mm wide and 10 mm deep) machined into it. A steel casing was braised on the copper block. A photograph and a scheme of the bottom terminations are shown in figure 6. Each staggered stack was soldered to the copper termination using eutectic SnPb at a temperature of about 200°C. Copper strips were inserted vertically in the grooves on the Hastelloy side of the stack in order to push the side of the tape with the superconducting ceramic in direct contact with the copper of the termination. On the termination that will be in contact with the HTS adapter, a transition copper block was used to bring the stacks close to each other (see figure 7), and fit in the available space. A photograph of the termination after soldering is presented in figure 8. After soldering a steel cover is welded on top and steel pipes are also welded to the terminations for cooling. Assuming a specific contact resistance of the tape on copper at 4.2 K of  $10^{-11} \Omega \cdot \text{m}^2$  (a conservative value, because on a test sample specific resistances between  $2 \cdot 10^{-12} \Omega \cdot \text{m}^2$  and  $6 \cdot 10^{-12} \Omega \cdot \text{m}^2$  were measured), the total resistance of each termination can be calculated by considering the parallel resistance between 320 identical tape to copper connections (over 4 mm x 15 mm contact area), obtaining about 0.5 n $\Omega$  for one termination.

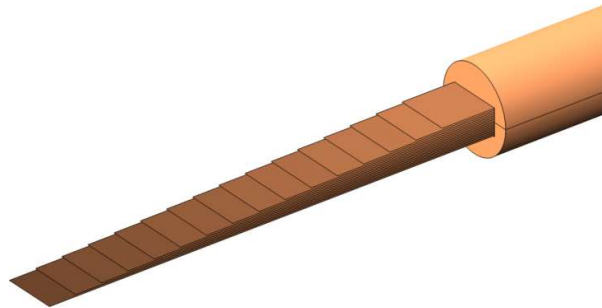


Figure 5. Schematic 3D model of the staggered tapes at the end of the strand.

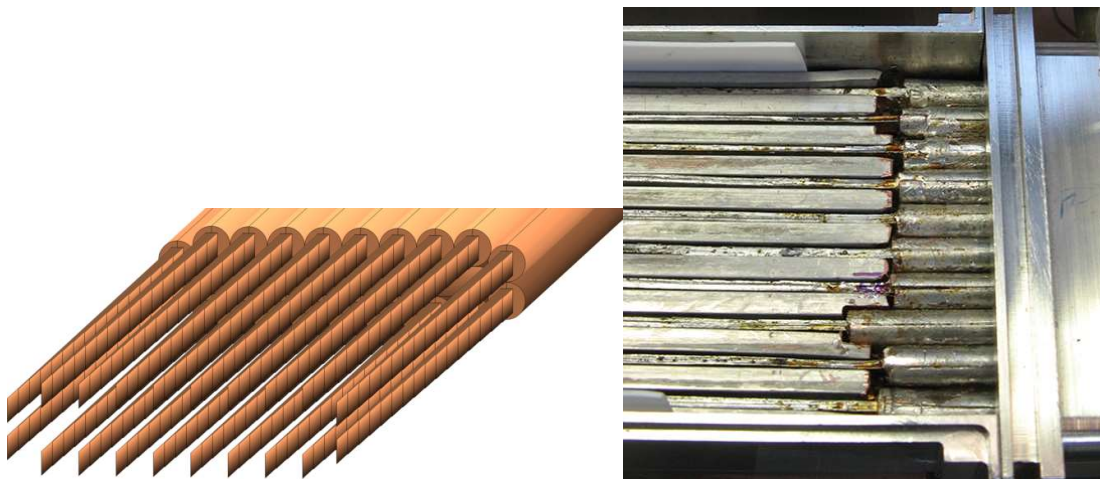


Figure 6. Left: schematic drawing of the bottom termination. Right: photograph of the bottom termination before soldering; the strands are visible on the right side.

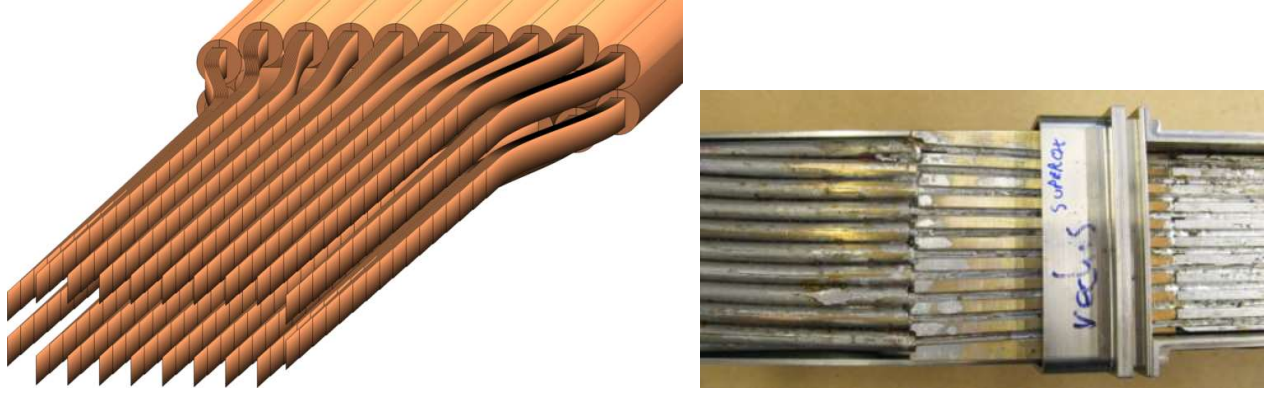


Figure 7. Left: schematic 3D model of the end of the cable at the top termination to be connected with the HTS adapter: the stacks are bent into a grooved copper piece before being inserted in the termination. Right: photograph of the grooved copper piece and termination after soldering.



Figure 8. Bottom termination after soldering. A steel cover will be welded to close the termination box.

#### 4. Assessment of the prototype's properties

The tape from Superox came in four spools, corresponding to four production runs. Short samples (4 cm long) were cut from each spool and the  $I_c$  measured at 77 K in self field and at 4.2 K, 12 T. From Superpower 23 spools were purchased; the characterization of all the spools was considered time consuming; therefore samples from 11 spools, corresponding to 65% of the total tape length, were tested at 77 K in self field and at 4.2 K, 12 T. For the remaining 12 spools (35% of the total tape length) the average lift factor was obtained from the measured spools (the values did not follow a normal distribution, but a log-normal instead) and it was used to extrapolate the values of  $I_c$  from 77 K to 4.2 K, 12 T. The nominal  $I_c$  at 4.2 K, 12 T of the two conductors is obtained by summing up the  $I_c$  of all the tapes: the values obtained are 62 kA  $\pm$  2 kA ( $\pm$ 3%) for the Superpower cable and 62 kA  $\pm$  1.5 kA (2%) for the Superox cable. Once the values at 4.2 K and 12 T are determined it is necessary to scale them to various temperatures and fields also taking into account the magnetic field generated by the return conductor, the self-field and the angular dependence.

The following scaling law is used to describe the field and temperature dependence:

$$I_c(B, T) = A \frac{B_o(T)^\beta}{B} \left( \frac{B}{B_o(T)} \right)^p \left( 1 - \frac{B}{B_o(T)} \right)^q$$

$$B_o(T) = B_o \left( 1 - \frac{T}{T_o} \right)^\alpha$$

The scaling law requires a set of 5 parameters ( $\alpha, \beta, p, q, B_o, T_o$ ) plus an additional parameter  $A$  for scaling the critical current. In order to increase the accuracy of the fit in the region of low temperatures (<40 K) and high fields (>8 T) only data points in that region were considered. The parameters should be considered simply as fitting parameters with no physical meaning, i.e.  $B_o$  and  $T_o$  should not be considered as the irreversible field and temperature. The Superox

scaling parameters were obtained by fitting the data for the tape (field perpendicular to the wide face of the tape) provided by the manufacturer and measured at ENEA. The Superpower parameters were obtained by fitting the data published in [11]; one of the Superpower tape used for the cable was measured also down to 8 T and it was found that the field dependence was slightly different from the field dependence of the tape measured in [11], while for the Superox tape used for the cable the field dependence is the same as the one measured by Superox/ENEA. The sets of data for Superpower and Superox and the corresponding fits are reported in figure 9.

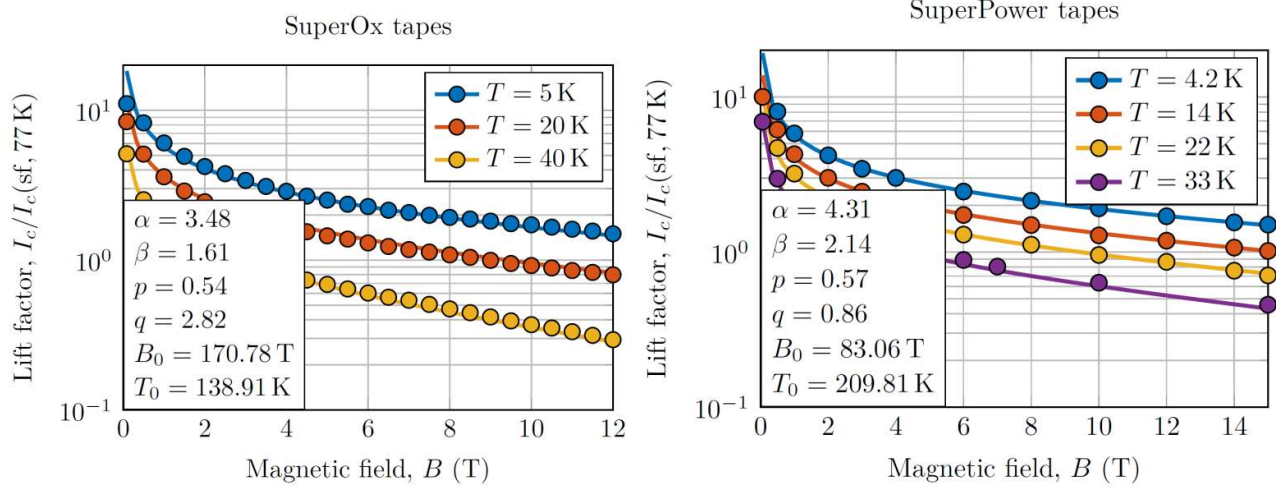


Figure 9. Reduced critical current versus field at different temperatures. Left: Superox tape measured at ENEA, Italy. Right: Superpower tape, data published in [11]. The fitting lines and the values of the fitting parameters are also reported.

The current sharing temperature and the critical current of the cables are calculated considering not only the background field, but also the self-field generated by the cable and the field generated by the return conductor. Comparison of the self-field distribution generated by one cable carrying 60 kA and by two cables carrying 60 kA in opposite directions and separated by 60 mm (as it is the case in the sample to be measured in EDIPO) is given in figure 10 (due to the symmetry, only half of the cross section is shown).

The real orientations of the stacks in the cable (see figure 10) and the angular dependence of the critical current (see figure 11) were also considered. According to the orientation of every single tape in the cable, the total magnetic field is separated in parallel  $B_\xi$  and perpendicular  $B_\eta$  components with respect to the wide face of the tape. The angle between the magnetic field and the wide face of the tape is equal to  $\theta = \arctan(B_\eta / B_\xi)$ . The tapes are twisted with 320 mm twist pitch and are arranged around the copper core. Average electrical field in the cable cross section  $E$  was obtained as a function of temperature (at fixed magnetic field distribution) using the following equation:

$$\frac{E(T)}{E_c} = \frac{1}{N_{mesh}nN} \sum_{(i,j,k)=1}^{N_{mesh}nN} \left( \frac{I}{I_c(B^{(i,j,k)}, T)} f(\theta^{(i,j,k)}) \right)^{n(B^{(i,j,k)}, T)}$$

where  $i$  indicate the mesh element in the tape,  $j$  the tape position in the strand and  $k$  the strand position in the cable;  $B^{(i,j,k)}$  is the magnitude of the total magnetic field, which includes the background field  $B_b$ , the self-field and the field of the return cable at  $(i, j, k)$  position.  $f(\theta)$  is an interpolation function obtained from the data in figure 11.



Finally  $T_{cs}$  is obtained as the solution of the equation  $E(T_{cs})=E_c$ , where  $E_c = 0.1$  or  $1 \mu\text{V}/\text{cm}$ . In general, the self-field and return field decrease the nominal critical current values, while the angular dependence of  $I_c$  is an improving factor, because the nominal  $I_c$  were measured at  $90^\circ$ . The effect of the self-field, return conductor field and angular dependence is less than 2% in the range 8 T to 10 T and 20 kA to 60 kA. The results of the calculations are given in the next section together with the results of measurements.

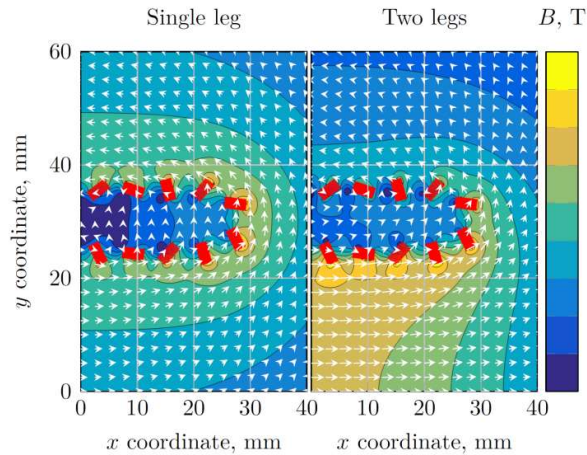


Figure 10. Left: Magnetic field profile generated by the conductor (self-field). Right: total magnetic field profile generated by the conductor (self-field) and by the return conductor.

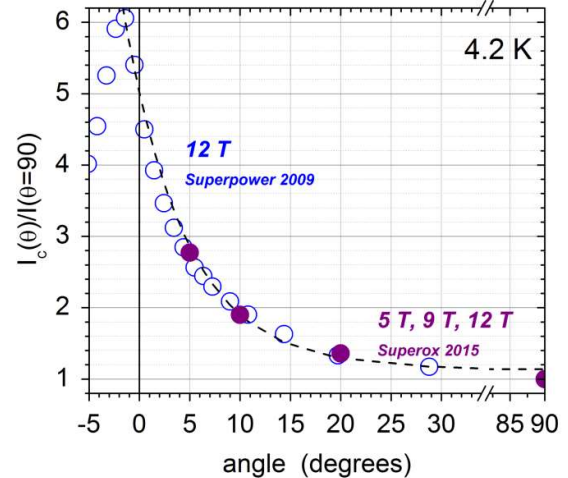


Figure 11. Superpower data are from [15]. Superox data have been measured on the tapes used for the cable at various field and angles.

## 5. Test in the EDIPO facility

The new EDIPO facility at the Swiss Plasma Center [16] is composed of a dipole generating up to 12.3 T with 1% homogeneity over 100 cm and of a superconducting transformer to feed samples with current up to 100 kA. For testing samples at temperatures exceeding 10 K a special “HTS adapter” was manufactured [17]. The adapter has a function similar to a current lead, providing superconducting current flow with a relatively high thermal resistance, so that the NbTi superconducting transformer is thermally decoupled from the sample to be measured. A counter flow heat exchanger was also installed in the hydraulic circuit of the sample; the heat exchanger is used to avoid sending warm helium back to the refrigeration plant. The commissioning of the adapter and heat exchanger will be presented in [18].

After jacketing the cables and soldering the terminations the two conductors were assembled in an EDIPO sample and connected to the HTS adapter; all joints were prepared with indium wires. On each conductor six pairs of voltage taps were spot welded to the steel jacket. Two pairs of thermometers (the temperature is measured with accuracy better than 50 mK) were also glued to the jacket on each conductor, outside the voltage taps. The full instrumentation scheme is sketched in figure 12. A cross section of the sample is shown in figure 13.

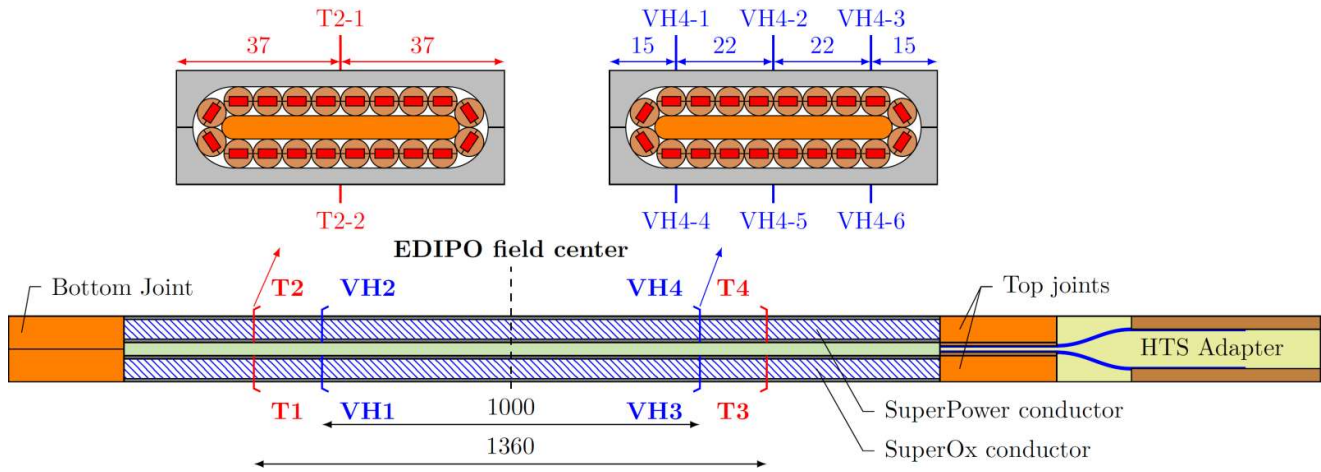


Figure 12. Scheme of the instrumentation for the two conductors. The current from the superconducting transformer flows from the adapter through one of the top joints into the conductor, then through the bottom joint and up in the second conductor, through the top joint back into the HTS adapter and to the transformer. Example cross section at the location of the thermometers and voltage taps are also shown.

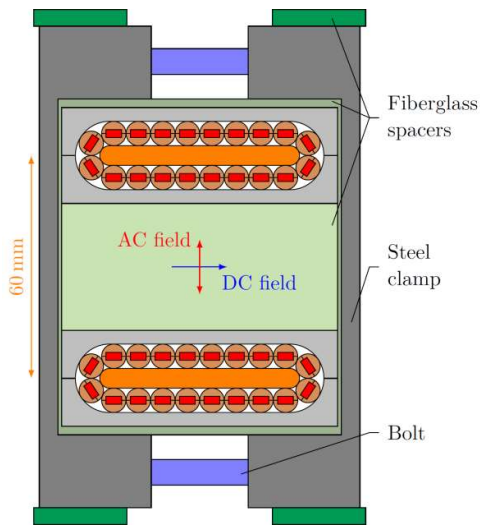


Figure 13. Cross section of the EDIPO sample. The two conductors are separate by a fiberglass spacer. Steel clamps hold the components. The directions of the background magnetic field (DC field) and of the alternating magnetic field (AC field, used for AC losses measurement) are also indicated.

### 5.1. DC tests

First the resistance of joints and terminations was measured up to 50 kA around 4.5 K and in zero background field; an example of a measurement run is shown in figure 14. The total bottom joint resistance (including the Superpower cable bottom termination, the SuperOx cable bottom termination and the joint between the two terminations) was less than 1 n $\Omega$ : one voltage tap located between the two terminations allows to split the components of the total resistance: the Superpower cable bottom termination, the joint between the copper blocks (indium wires) and the SuperOx cable bottom termination have all the same resistance of about 0.3 n $\Omega$  each. The resistance of the Superpower top joint (cable termination plus indium joint) was about 2 n $\Omega$  while the resistance of the SuperOx top joint (cable termination

plus indium joint) was about 1 n $\Omega$ . The total resistance of the circuit was about 10 n $\Omega$ , most of it coming from the HTS adapter.

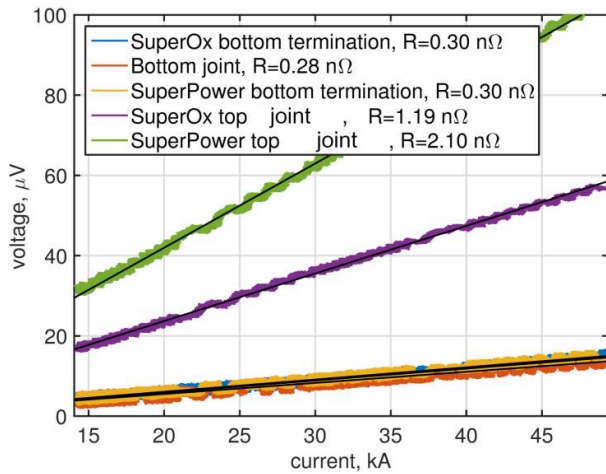


Figure 14. Voltage versus current relations measured on the joints and terminations at 4.2 K in zero background magnetic field.

The test program was similar to the one used for the qualification of the ITER TF conductors: the current sharing temperature is measured by setting a fixed background magnetic field and a fixed current in the sample and then increasing gradually the temperature of the helium flow with a continuous ramp. For the critical current measurement, field and temperature are fixed and the current is gradually increased; in this kind of operation the repetition of  $I_c$  tests at exactly the same temperature is almost impossible because the precise setting of the temperature is very difficult.

In most of the ITER TF conductors the offset among the six pairs of voltage taps increases from zero to few microvolts during the current ramp till 68 kA. Instead, in the HTS cable prototypes, the offset among the six pairs of voltage taps remains constant (within the accuracy of the measurement) during the ramps in current: this is an indication that the cable cross section is an equipotential surface and that the current distribution among strands in the cable cross section is uniform. In the following plots the average electric field is the average of the six pairs of voltage taps; in a similar way the average temperature is the average value of the four thermometers and the typical standard deviation of the mean is less than 1%, for example  $\pm 0.05$  K for a  $T_{cs}$  of 7 K and  $\pm 0.25$  K for a  $T_{cs}$  of 35 K .

Examples of the  $E-T$  transitions are shown in figure 15a: in the measurement at high currents (for example 60 kA) the base line was not visible because the superconducting transition starts at temperature lower than 4.5 K; the offset of the voltage was estimated by fitting the data with  $E = E_{offset} + E_c \cdot (T/T_{cs})^m$ ; the same procedure was used also with measurements at low current (for example 30 kA, as shown in figure 15a) and it was confirmed that the offsets obtained by fitting are comparable to the actual ones. The exponential  $m$  value is introduced in the  $E-T$  characteristics at constant current and magnetic field in analogy with the exponential  $n$  value which is used to characterise the steepness of the  $E-I$  characteristics at constant temperature and magnetic field. In figure 15b the  $E-T$  characteristics are reported for the SuperOx cable in background field of 12 T and at currents from 20 kA up to 60 kA; the corresponding exponential  $m$  values are also reported. Similar curves were observed at 10 T and 8 T background fields. In figure 15c the exponential  $m$  values are plotted together with the expected  $m$  values obtained from applying the scaling laws to the short sample measurements. Relatively low  $m$  values are expected because of the intrinsic properties of coated conductor (i.e. very high critical temperature); only the operation at low current can guarantee a sharper transition.

While the  $m$  values measured at 12 T follow the expected trend, the values measured at 8 T and 10 T are lower than the expected ones. In contrast with Nb<sub>3</sub>Sn conductors, it could be possible to operate HTS conductors at currents close to the critical current still retaining a sufficient temperature margin, but the superconducting transition will be relatively shallow. During the E-I test at 12 T the exponential  $n$  value was found to be about 12 at a temperature of about 6 K; despite the critical current was within 2% from the values of short sample, the exponential  $n$  value is smaller, than the ones (between 30 and 40) measured in tapes at 12 T, 4.2 K.

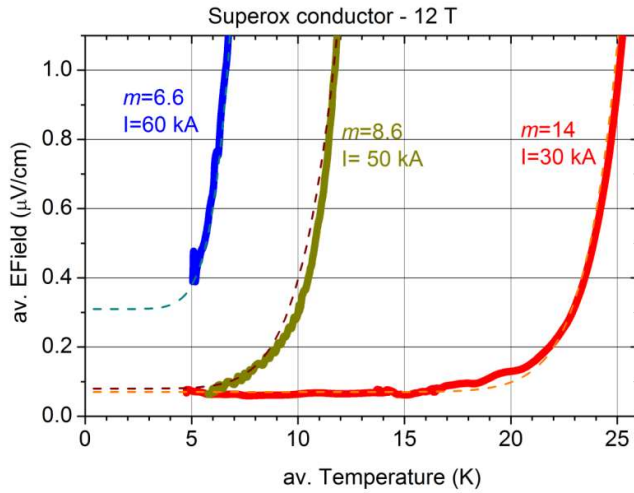


Figure 15a. Electric field versus temperature measured on the Superox conductor at 12 T and various operating currents. The fits with  $E = E_{\text{offset}} + (T/T_{cs})^m$  are also shown.

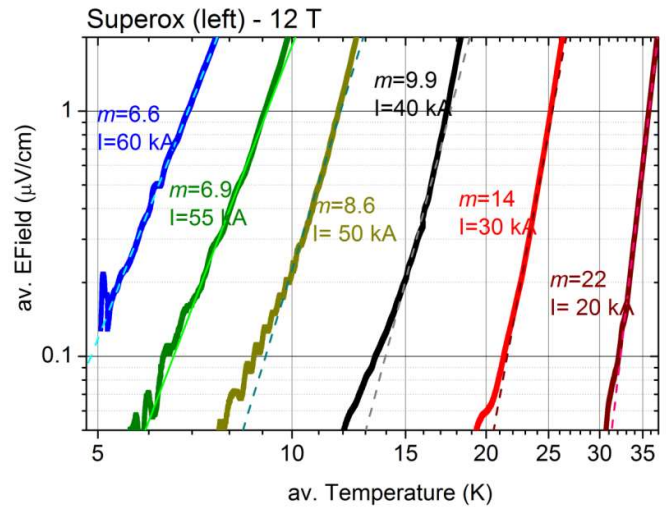


Figure 15b. Electric field versus temperature measured on the Superox conductor at 12 T and various operating currents.

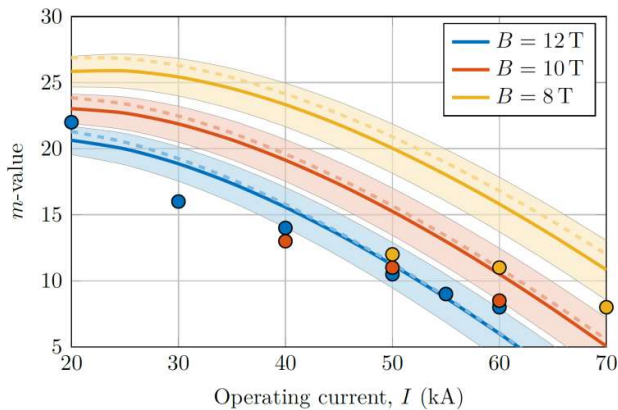


Figure 15c. Measured exponential  $m$  values (points) and expected ones (lines) for the Superox conductor.

In figure 16a the current sharing temperatures and critical current measurements are summarized for the Superox conductor; the bands indicate an error of  $\pm 2\%$  which comes from the propagation of the error on the critical current of the cable at 4.2 K, 12 T (see “Assessment of the prototype’s properties”). In figure 16b the values at 0.1  $\mu\text{V}/\text{cm}$  are also reported but the assessment of the  $T_{cs}$  values at 0.1  $\mu\text{V}/\text{cm}$  was not carried out because the data for the determination of the parameters at 0.1  $\mu\text{V}/\text{cm}$  are not available. The same plots for the Superpower conductor are in figure 17a and 17b; the bands in the case of the Superpower conductor indicate an error of  $\pm 3\%$ . The error on the measured  $T_{cs}$  is less than 1%, smaller than the size of the points in the figure. For both conductors the measured values

lies within few percent from the expected values at least in the region close to 4.2 K 12 T, where the tapes were measured; at much higher temperature or, in the case of Superpower conductor, at lower field the deviation of the measured values from the expected ones is probably due to the inaccuracy of the fitting parameters of the scaling laws.

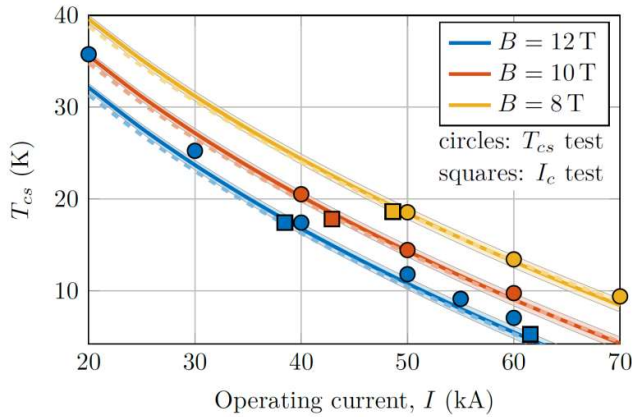


Figure 16a. Current sharing temperatures and critical currents at various background magnetic fields and operating currents for the Superox conductor. Lines are for the expected values. The criterion is 1  $\mu\text{V}/\text{cm}$ .

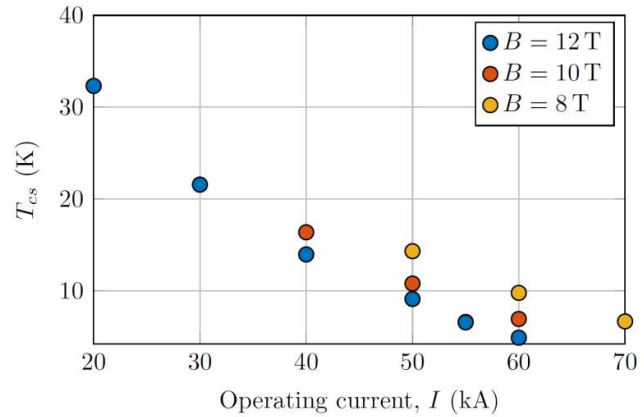


Figure 16b. Current sharing temperatures and critical currents at various background magnetic fields and operating currents for the Superox conductor. The criterion is 0.1  $\mu\text{V}/\text{cm}$

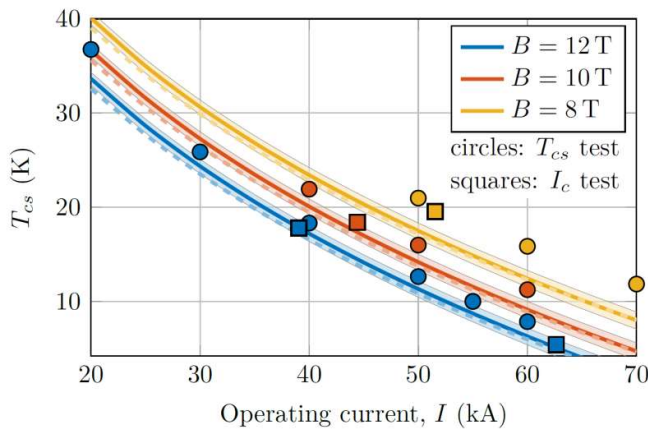


Figure 17a. Current sharing temperatures and critical currents at various background magnetic fields and operating currents for the Superpower conductor. Lines are for the expected values. The criterion is 1  $\mu\text{V}/\text{cm}$ .

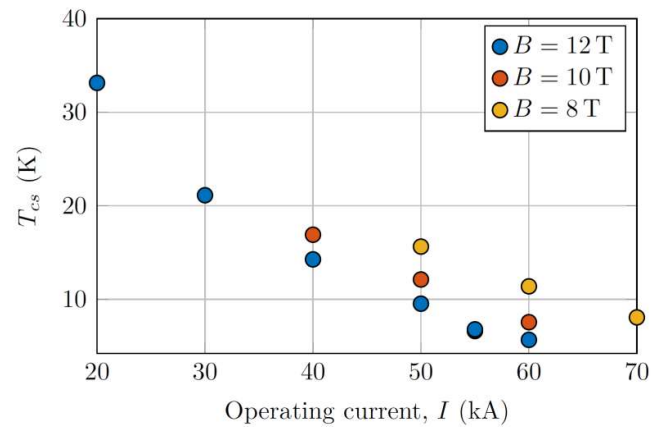


Figure 17b. Current sharing temperatures and critical currents at various background magnetic fields and operating currents for the Superpower conductor. The criterion is 0.1  $\mu\text{V}/\text{cm}$ .

After the initial set of measurements summarized in figure 16a/b and figure 17a/b, during which the current in the conductors was ramped about 20 times, the conductors went through electromagnetic cycling, consisting in ramping the current from zero to 50 kA and back to zero in a background field of 12 T. In this way transverse electromagnetic forces as large as 750 kN per meter of cable are applied to both conductors, corresponding to a pressure of about 10 MPa over the width of the cable. After 100 cycles the  $T_{cs}$  at 12 T and 50 kA was measured again; the measurement was repeated after 500 and 1000 cycles. The  $E$ - $T$  curves for the Superox conductor at various electromagnetic cycling are shown in figure 18; the reduction in  $T_{cs}$  is accompanied by a reduction of the exponential  $m$  value. The Evolution

of  $T_{cs}$  with the number of cycles is plotted in figure 19 for both conductors (at 0.1  $\mu\text{V}/\text{cm}$  and 1  $\mu\text{V}/\text{cm}$ ). The reduction of about 10% after 1000 cycles that is observed in  $T_{cs}$  would correspond to a reduction in critical current of about 3%, because of the very high critical temperature of coated conductors (see figure 1). This is very difficult to be measured because in the critical current measurements the temperature cannot be controlled with a precision high enough to detect few % of variation in  $I_c$ . A reduction of 3% or 4% in  $I_c$  could be due to the damage of some of the tapes/strands, but it is also compatible with a change in strain up to about  $\epsilon=0.4\%\sim 0.45\%$  for all the strands [19]. At the moment it is not possible to identify the reason of the reduction of  $T_{cs}$ , but further tests and electromagnetic cycling are planned after a warm-up cool-down; eventually the disassemble, inspection and test of the individual strands will be carried out at the end of the test campaign in EDIPO.

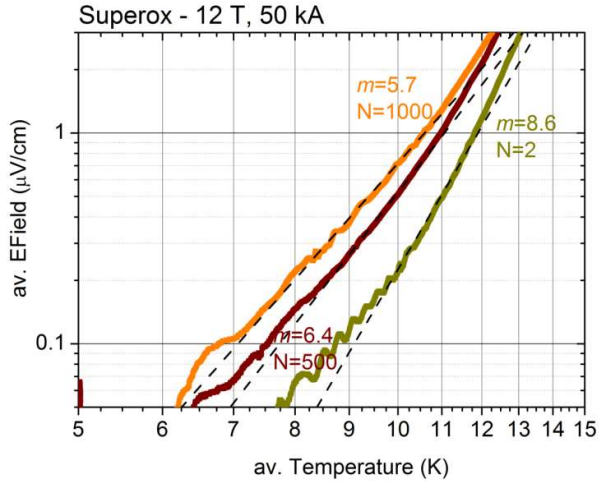


Figure 18. E-T curves for the SuperOx conductor in the initial set of measurements ( $N=2$ ) and during the electromagnetic cycling ( $N=500, 1000$ ) at 12 T, 50 kA. The  $m$  value is also indicated.

### 5.2. AC tests

The AC losses were measured on the two prototype conductors just before and after the DC test. The test program was similar to the one that is used for the qualification of the ITER TF conductors: a background field of 2 T is applied in order to suppress the superconductivity in the solder alloy, and then an AC field is superimposed. The main difference with respect to the SULTAN facility is that in EDIPO the AC coils cover a length of 1.6 m instead of 0.4 m. The total AC losses of the cables have been measured using a calorimetric method: first the power loss  $P$  released in the He flow is measured and then the energy loss per cycle  $Q$  is calculated from  $P$  using:

$$P = (h(T_{out}, p) - h(T_{in}, p)) \frac{dm/dt}{l} \quad [W/m]$$

$$Q = P/\nu \quad [J/m/cycle]$$

where  $T_{in}$  is the average value measured by thermometer T2-1 and T2-2,  $T_{out}$  is the average value measured by thermometer T4-1 and T4-2 (see instrumentation scheme in figure 12),  $p$  is the absolute pressure,  $dm/dt$  the mass flow rate,  $l$  the distance between temperature sensors (1.36m) and  $\nu$  the frequency of the AC field. The enthalpy of the helium as function of temperature and pressure was obtained by the interpolation of tabulated data [20]. The

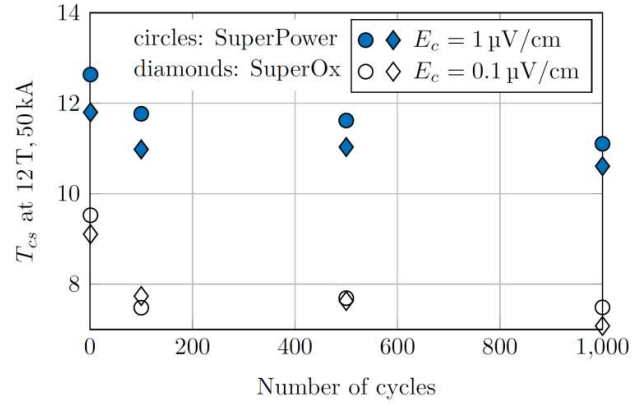


Figure 19. Evolution of the current sharing temperature at 50 kA and 12 T for the two conductors during electromagnetic cycling. The criterion is 1  $\mu\text{V}/\text{cm}$ .

calorimetric method doesn't work well at low frequencies, thus the lowest frequency used with the method was  $\nu=0.05$  Hz.

After the AC field is applied the temperature of the He flow increases and reaches a plateau, as shown in figure 18. In order to get rid of the oscillations in the temperature, which follows the oscillations of AC field, the temperature signal was fitted with the following analytical model:

$$\begin{aligned}
 t < t_1 &: y = T_1 \\
 t_1 < t < t_2 &: y = T_1 + (T_2 - T_1)(1 - e^{-\alpha_1(t-t_1)}) \\
 t > t_2 &: y = T_3 + \left( T_1 - T_3 + (T_2 - T_1)(1 - e^{-\alpha_1(t_2-t_1)}) \right) e^{-\alpha_2(t-t_2)}
 \end{aligned}$$

The model contains in total 7 adjustable parameters:  $(t_1, t_2, \alpha_1, \alpha_2, T_1, T_2, T_3)$ . An example of the temperature signals during a test and the corresponding fits (black lines) are shown for both conductors in figure 20.

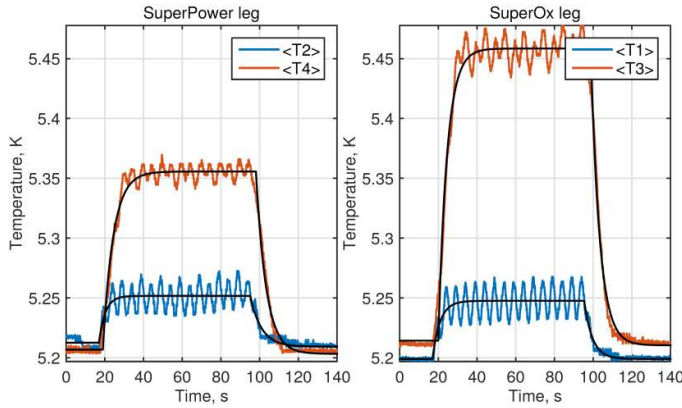


Figure 20. Inner temperature and outer temperature of the He flow during a test with AC fields of 0.3 T. The AC field is switched on at  $t=20$  s and switched off at  $t=100$  s.

Measurements were carried out with AC amplitude values of 0.1 T, 0.2 T and 0.3 T; all these data have been rescaled to 0.3 T and plotted together in figure 21a; for comparison the values of an ITER TF conductor (TFJA8) are also reported.

The values of the hysteretic AC losses can be obtained by extrapolating the measured values down to zero frequency (see figure 21b). For the ITER TF the hysteretic losses are about 10 J/m, while in the HTS prototype they are estimated to be between 5 and 10 J/m for the Superpower conductor and between 15 and 30 J/m for the Superox conductor. The hysteretic losses are proportional to the dimension of the superconducting layer (in both Superpower and Superox tapes the ceramic is 4 mm wide and 1 to 1.5 microns thick) and to the critical current density. A possible explanation for the difference between the two cables, at least qualitatively, is that at the measurement conditions (2 T and 4.5 K) the superconducting current density of the tapes of the Superox cable is about 40% higher than the one of the tapes of the Superpower cable. The hysteretic losses per unit of volume can be calculated assuming a total cross section of the superconducting REBCO ceramic of about  $4 \text{ mm}^2$  and a total cross section of the  $\text{Nb}_3\text{Sn}$  phase of about  $50\sim 70 \text{ mm}^2$ . Therefore the hysteretic losses per cycle becomes  $1\sim 8 \text{ J/mm}^3$  for the HTS cable prototypes and  $0.1\sim 0.2 \text{ J/mm}^3$  for ITER TF cables. The higher values in the HTS prototype are due to the larger dimension of the superconducting layer, up to 4 mm, in contrast with filament diameters of few microns for the  $\text{Nb}_3\text{Sn}$  strands in the ITER TF conductor.

The hysteretic losses represent only a fraction of the total losses, the main contribution coming from coupling losses. Coupling losses can have two different sources: losses in the strands (coupling among the 16 tapes in the stack) and losses in the cable (coupling among strands). The lower total losses observed in the Superpower cable can be due to the fact that the contact between the strands is reduced, in fact in the Superpower cable the core was a bit too large and copper strips were inserted between the strands to fill up the gaps; therefore the higher contact resistance would decrease the amplitude of the coupling currents. In the Superox cable the inter-strand resistance is somehow lower (the strands are tightly packed), and the coupling losses are larger than in the Superox cable.

A small reduction of the AC losses after the electromagnetic cycling is observed in the Superox cable especially at low frequency, suggesting that it is somehow related to the hysteretic losses, but a clear explanation is not yet found.

The total losses in the prototype cables are larger than in the ITER TF cables; whether they are still acceptable, depends on the cryogenic analysis of the whole magnet system, including the nuclear heat. Nevertheless the coupling losses at the strand level can be reduced by using a solder alloy with higher electrical resistance; the coupling losses at cable level can be reduced by plating the copper core so that the current loops cannot flow through the core.

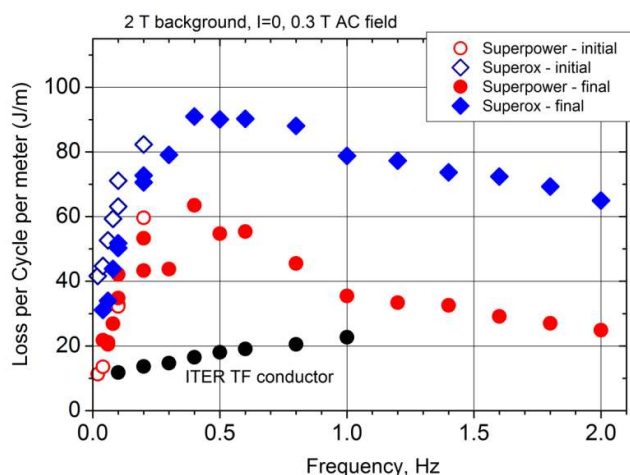


Figure 21a. Total AC losses as a function of the AC field frequency for the two prototype conductors. The ITER TFJA8 conductor is also reported for comparison.

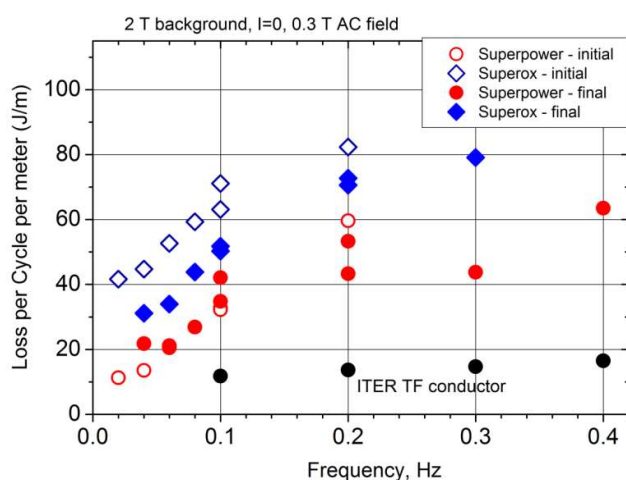


Figure 21b. Enlargement of fig 21a. This is used for estimating the hysteretic losses with a linear extrapolation to zero frequency.

## 6. Summary

Two cable prototypes were manufactured at laboratory scale and tested in fields up to 12 T in the EDIPO facility. Both cables could carry currents of 60 kA at 5 K and 12 T background field. Initially the measured critical currents and current sharing temperatures were within few percent of the values measured on samples of the tapes used for the manufacturing: the superconducting transport properties of the tapes were fully retained in a large cable composed of partially transposed strands.

During cycling under transverse load (750 kN per meter of cable) a reduction of  $T_{cs}$  was observed, reaching 10% after 1000 cycles. The value would correspond to about 3% of reduction in critical current. The reason for the reduction of  $T_{cs}$  during electromagnetic cycling is not yet identified, but further tests and investigations are planned.

The measurement of the AC losses was also carried out: the values are from 2 to 10 times larger than in the ITER TF conductors, but various possibilities exist for a reduction.



## 7. References

- [1] Devred A *et al* 2014 Challenges and status of ITER conductor production *Supercond. Sci. Technol.* 27 044001
- [2] Komarek P 2006 Potential and desire for HTS application in thermonuclear fusion *Fusion Engineering and Design* 81 2287-2296
- [3] Takayasu M *et al* 2012 HTS twisted stacked-tape cable conductor *Supercond. Sci. Technol.* 25 014011
- [4] Schlachter S I *et al* 2011 Coated Conductor Rutherford Cables (CCRC) for High-Current Applications: Concept and Properties *IEEE Trans. Appl. Supercond.* 21 3021-4
- [5] van der Laan D C *et al* 2011 Compact GdBa<sub>2</sub>Cu<sub>3</sub>O<sub>7- $\delta$</sub>  coated conductor cables for electric power transmission and magnet applications *Supercond. Sci. Technol.* 24 042001-4
- [6] Terazaki Y *et al* 2015 Measurement and analysis of critical current of 100-kA class simply-stacked HTS conductors *IEEE Trans. Appl. Supercond.* 25 6977909
- [7] Uglietti D, Wesche R and Bruzzone P 2013 Fabrication trials of round strands composed of coated conductor tapes *IEEE Trans. Appl. Supercond.* 23 6410385
- [8] Uglietti D, Wesche R and Bruzzone P 2014 Design and Strand Tests of a Fusion Cable Composed of Coated Conductor Tapes *IEEE Trans. Appl. Supercond.* 24 4800704
- [9] Uglietti D *et al* 2015 Development of HTS Conductors for Fusion Magnets *IEEE Trans. Appl. Supercond.* 25 6937173
- [10] Bykovsky N *et al* 2015 Strain Management in HTS High Current Cables *IEEE Trans. Appl. Supercond.* 25 4800304
- [11] Lombardo V *et al* 2011 Critical Currents of YBa<sub>2</sub>Cu<sub>3</sub>O<sub>7</sub> Tapes and Bi<sub>2</sub>SrCa<sub>2</sub>Cu<sub>2</sub>O<sub>x</sub> Wires at Different Temperatures and Magnetic Fields *IEEE Trans. Appl. Supercond.* 21 3247-3250
- [12] Bruzzone P *et al*. "Design of Large Size, Force Flow Superconductors for DEMO TF Coils", *IEEE Trans. Appl. Supercond.*, vol. 24, 2014, 4201504.
- [13] Hahn S *et al* 2015 Design Study on a 100-kA/20-K HTS Cable for Fusion Magnets *IEEE Trans. Appl. Supercond.* 25 4801605
- [14] Bykovsky N *et al* 2014 Analysis of critical current reduction in self-field in stacked twisted 2G HTS tapes *Journal of Physics: Conference Series* 507 022001
- [15] Uglietti D *et al* 2009 Angular Dependence of Critical Current in Coated Conductors at 4.2 K and Magnet Design *IEEE Trans. Appl. Supercond.* 19 2909-2912
- [16] Bruzzone P *et al* 2014 Commissioning of the Main Coil of the EDIPO Test Facility *IEEE Trans. Appl. Supercond.* 24 9500205
- [17] Wesche R *et al* 2013 Prospects for the use of high-T<sub>c</sub> superconductors in fusion magnets and options for their test in SULTAN *Fusion Engineering And Design* 88 1495-1498
- [18] Wesche R *et al* 2015 Commissioning of HTS adapter and heat exchanger for testing of high current HTS conductor *to be presented at EUCAS 2015*
- [19] Barth C *et al* 2015 Electro-mechanical properties of REBCO coated conductors from various industrial manufacturers at 77 K, self-field and 4.2 K, 19 T *Supercond. Sci. Technol.* 28 045011
- [20] Van Shiver S W, Helium cryogenics (Springer New York, New York, NY, 2012)